Proceedings of the 17th IEEE International Symposium on Robot and Human Interactive Communication, Technische Universität München, Munich, Germany, August 1-3, 2008

Vision System for Wearable and Robotic Uses

Erich Schneider, Stefan Kohlbecher, Thomas Villgrattner, Klaus Bartl, Stanislavs Bardins, Tony Poitschke, Heinz Ulbrich, Thomas Brandt ‡

Abstract

Visual perception is thought to provide us with the illusion of a stable visual world that is seamless in time and space while it is continuously explored with saccades. The oculomotor system ensures retinal image stabilization during head, object, and surround motion. Prior to manipulation, objects are fixated with top-down driven look-ahead saccades, and similarly, the locomotion path is visually inspected about two steps ahead. In human-human interaction tasks gaze is not only crucial for motor intention recognition but it is also essential in detecting the direction of social attention.

A new prototype of a camera motion control unit was developed that provides a sufficiently short latency and a light-weight setup for both a wearable gaze-controlled and a humanoid stereo camera system. The camera system will serve as a binocular eye plant for a humanoid active vision system. The long-term aim is to integrate eye tracking capabilities into the vision system that will equip the humanoid with the ability to infer the target of gaze of a human in human-machine cooperation scenarios. The eye tracking technology has been improved by extending it into the direction of a calibration-free operation. The antropomorphic camera motion control system was integrated into the humanoid JOHNNIE*. Thereby, a new experimental tool was created that will help to evaluate the relevance of gaze and look-ahead fixations in the interaction of humans with humanoids in social contexts or during (humanoid) locomotion.*

*This work was supported in part within the DFG excellence initiative research cluster Cognition for Technical Systems

†E. Schneider, S. Kohlbecher, K. Bartl, S. Bardins, and T. Brandt are with the Dept. of Neurology, Ludwig-Maximilians University of Munich, 81366 Munich, Germany eschneider@nefo.med.uni-muenchen.de

‡T. Villgrattner, H. Ulbrich are with the Institue of Applied Mechanics, T. Poitschke is with the Institute for Human-Machine Communication, Technische Universität München, Munich, Germany

1. INTRODUCTION

Visual perception provides us with the illusion of a stable visual world that is seamless in time and space while it is continuously explored with saccades, and while the oculomtor system ensures retinal image stabilization during head, object, and surround motion [1]. Prior to manipulation, objects (workpieces) are fixated with top-down driven look-ahead saccades [2], and similarly, the locomotion path is visually inspected about two steps ahead [3]. During vehicle driving the steering angle is correlated with and preceded by the angle of gaze [4]. In dual task scenarios, gaze is also a reliable indicator of attention switching between the tasks [4]. In human-human interaction tasks the direction of gaze is not only crucial for motor intention recognition [5] but it is also essential in detecting the direction of social attention [6]. Gaze is therefore important in everyday human activities and in human-human interactions as a modality of proactive or look-ahead information gathering for action planning. We present a first step in our attempt to bring this level of interaction to human-machine scenarios.

There are attempts to technically replicate ocular motor function [7, 8], but currently there is no freely moving humanoid vision system available, that integrates active visual exploration by saccades with vergence, accomodation, and 3D image stabilization during head, object, and surround motion by vestibulo-ocular, smooth pursuit, and optokinetic eye movements. Human ocular motor control incorporates all these functions, but so far no man-made vision system has replicated them completely. In [8], for example, a binocular system is presented that can perform horizontal disconjugate vergence movements, but in the vertical direction the system is restricted to conjugate movements only. In contrast, human eye movements, termed skew deviation, can also be vertically disconjugate [1]. Similarly, the mechanics presented in [7] can perform binocularly independent movements, however, the control computations are performed for the right eye only, while the left eye performs exactly the same motion.

978-1-4244-2213-5/08/$25.00 ©2008 IEEE

The mechanical setup of a camera actuation system has been developed that is able to reproduce the whole human oculomotor range in terms of functionality and dynamics. Together with a remote eye tracking system the current technical implementation will contribute to seamless gaze-based interactions between humans and machines (humanoids).

1.1. Applications

The newly developed camera orientation device will be used in two different applications:

1. As an active vision system for humanoid robots (see Figure 1) with the ability to track the eyes of a human in a human-machine cooperation scenario
2. In a head-mounted gaze-controlled camera (see Figure 2)

The gaze-controlled camera (*EyeSeeCam*) has been presented before [9]. In this paper we will therefore focus on the camera orientation device and on the remote eye tracking capabilities and their respective results. As far as *EyeSeeCam* (see Figure 2) is concerned, we will only report in the Results section the important measures for the total system delay that we obtained with the newly integrated camera orientation device.

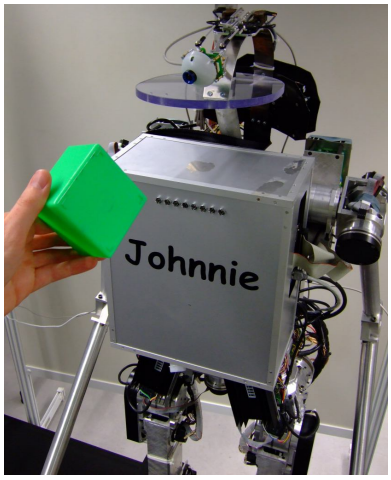

Figure 1. *JOHNNIE's* "'eye"' pursues a target

2. CAMERA ORIENTATION DEVICE

The aim of the presented system is to enable a seamless collaboration between humans and humanoid robots, such as *JOHNNIE* [10] and *LOLA* [11]. Human gaze direction is an important factor in accessing information about human intention, state, and learning behavior. Since under normal conditions a human operator can freely move, a stationary gaze-tracker is not

Figure 2. *EyeSeeCam* gaze-controlled head-mounted camera. Eye tracker signals are used to align a camera orientation device with gaze.

appropriate. In the presented approach the gaze-tracker cameras are mounted directly on the robot's head. In order to follow the human's eyes, pivotable cameras are used as robotic "eyes".

2.1. Requirements

In order to track a human eye the presented camera orientation device must reach the dynamic properties of the human ocular motor system. High velocities and accelerations of about 500 deg/s and 5000 deg/s^2, respectively, as well as short latencies are required [1]. The workspace of the camera orientation device should be about $\pm 30^\circ$ for both horizontal and vertical axis. Moreover, a light-weight and compact system is required.

2.2. Design of the device

The developed device can orient a camera around its horizontal (tilt) and its vertical (pan) axis. It consists of a small parallel kinematic with a backlash-free gimbal joint that is driven by piezo actuators. In order to reduce the inertia of the moving parts a parallel kinematic has been chosen, at the cost of a more complex mechanism with respect to a serial kinematic [12]. A CAD drawing of the presented device, with a denotation of the most important parts, is shown in Figure 3

High velocities and high accelerations are basic requirements to the actuators, but they must also be small and light-weight. New piezo actuators were chosen be-

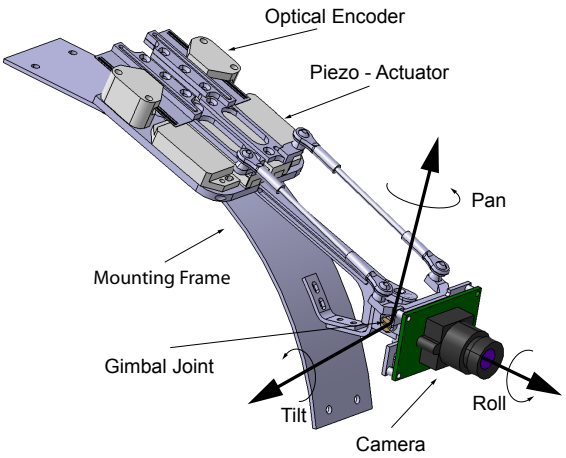

Figure 3. CAD model of the mechanical setup

cause they provide almost ideal properties for the intended applications. They are gear-less and they provide backlash-free movements. The possible velocities exceed those required by the oculomotor system and at low speeds the force/torque is high. In order to be able to set up a closed loop controller, position sensors were required. Small and lightweight incremental optical encoders were used (see Figure 3).

3. REMOTE EYE TRACKING

The second line of activities included the design of a new remote eye tracker, i.e., an eye tracker that can operate from a distance and that doesn't require any head-mounted devices. Since the development of the new eye tracking algorithms that we present here were done in parallel with the development of the camera orientation device, in a first step we used stationary stereo cameras. Future work will include the additional coordinate transformations that are required by an eye tracker that will use the camera orientation device.

Since modern eye tracking systems always need some sort of calibration, an eye tracking system that operates free of calibration would constitute a significant improvement. One approach to address this problem is reconstructing the pupil in 3D space and assuming that gaze direction parallels the pupil normal. If the position of the camera rig is known, this approach works without the need for a calibration procedure, because the position and orientation of the pupil ellipse is explicitly known. Since the assumption of collinearity between gaze and pupil normal does not hold [13], the calibration of the primary position is nevertheless required.

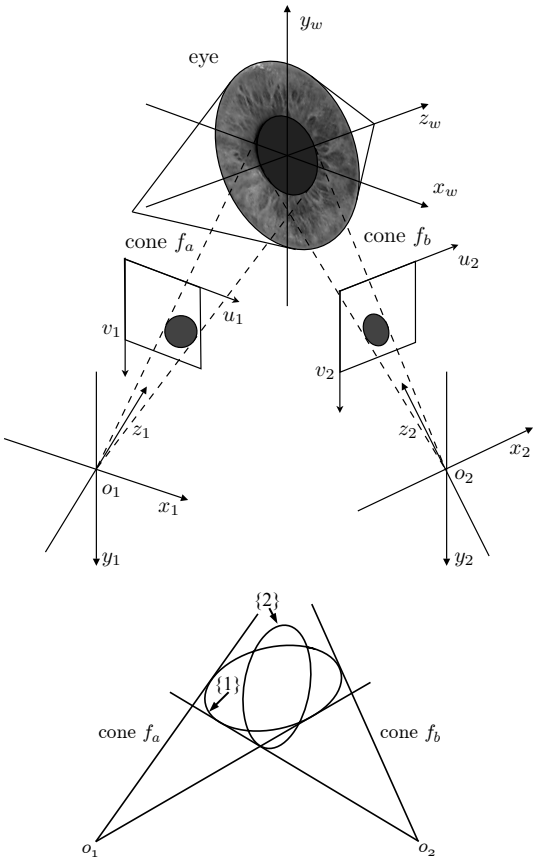

Figure 4. Coordinate systems and two images of the pupil (top) as well as the intersections of two cones (bottom)

3.1. Stereo reconstruction

The image of a circular pupil in the image plane is an ellipse. By laying a cone f_a through the camera center and the pupil image alone, one cannot determine the 3D position and orientation of the pupil, because many pupils are projected onto the same conic in the image plane. The situation changes if there is another projection of the same pupil on a second image plane. Now we can ray another cone f_b through the second camera center and pupil image. The intersection between the two cones then defines the pupil.

By reconstructing the original pupil ellipse from both projections, we can get position, size and orientation of the pupil in 3D space. A closed form solution to this problem has been proposed previously [14].

Figure 4 shows the image planes, the camera centers (o_1, o_2), the cones (f_a, f_b) and their intersection, and the pupil. The pupil is in the plane defined by the vectors x_w and y_w. The projections of the pupils are in

the normalized image planes, defined by the vectors u_1 and v_1 as well as u_2 and v_2. If the original pupil is assumed as an ellipse (or a circle), its projection results in an ellipse again, because projective transformations applied to conic sections always result in conic sections again. The projected ellipses are defined by the two conics:

$$\mathbf{x}^T\mathbf{A}_1\mathbf{x} = 0 \quad \text{and} \quad \mathbf{x}^T\mathbf{A}_2\mathbf{x} = 0 \tag{1}$$

Given the raw ellipse data, which is the lengths of both the semi-axis a and b, the position in the image plane t_x and t_y as well as the angle ϕ between the x-axis of the image plane and the first main axis of the ellipse, we can obtain the conic matrix by applying an affine transformation $\mathbf{S}$ to a conic $\mathbf{H}$ in normal form as follows:

$$\mathbf{A} = \mathbf{S}^T\mathbf{H}\mathbf{S} \tag{2}$$

$$\mathbf{S} = \begin{pmatrix} \cos\phi & -\sin\phi & -t_x\cos\phi + t_y\sin\phi \\ \sin\phi & \cos\phi & -t_x\sin\phi - t_y\cos\phi \\ 0 & 0 & 1 \end{pmatrix} \tag{3}$$

$$\mathbf{H} = \begin{pmatrix} \frac{1}{a^2} & 0 & 0 \\ 0 & \frac{1}{b^2} & 0 \\ 0 & 0 & -1 \end{pmatrix} \tag{4}$$

The relation between the coordinate system c_i of camera i and the world coordinate system c_w is:

$$\mathbf{x}_i = \mathbf{R}_i\mathbf{x}_w + \mathbf{t}_i \qquad i = 1,2 \tag{5}$$

For points in the pupil plane $\mathbf{x} = \begin{pmatrix} x_w, y_w, 0 \end{pmatrix}^T$ this can be written as:

$$\mathbf{x}_i = \mathbf{G}_i\mathbf{u}_w \qquad i = 1,2 \tag{6}$$

with $\mathbf{u}_w = \begin{pmatrix} x_w & y_w & 1 \end{pmatrix}^T$ being homogenous coordinates on the pupil plane and $\mathbf{G}_i$ being a 3×3 matrix consisting of the first two columns of $\mathbf{R}_i$ and the translation vector $\mathbf{t}_i$.

$$\mathbf{G}_i = \begin{pmatrix} \mathbf{r}_{i1} & \mathbf{r}_{i2} & \mathbf{t}_i \end{pmatrix} \tag{7}$$

With $u_i = \frac{x_i}{z_i}$ and $v_i = \frac{y_i}{z_i}$ follows:

$$z_i\mathbf{u}_i = \mathbf{G}_i\mathbf{u}_w \qquad i = 1,2. \tag{8}$$

An ellipse in the pupil plane is defined by

$$\mathbf{Q} = \begin{pmatrix} \frac{1}{a^2} & 0 & 0 \\ 0 & \frac{1}{b^2} & 0 \\ 0 & 0 & -1 \end{pmatrix} \quad \text{and} \quad \mathbf{u}_w^T\mathbf{Q}\mathbf{u}_w = 0 \tag{9}$$

Figure 5. Image processing output (left) and scene view from above (right)

and its projections by

$$\mathbf{u}_i^T\mathbf{A}_i\mathbf{u}_i = 0 \qquad i = 1,2 \tag{10}$$

Inserting (8) in (10) yields:

$$\mathbf{u}_w^T\mathbf{G}_i^T\mathbf{A}_i\mathbf{G}_i\mathbf{u}_w = 0 \qquad i = 1,2 \tag{11}$$

As equation (9) and (11) define the same conic $\mathbf{Q}$ we can write:

$$\mathbf{G}_i^T\mathbf{A}_i\mathbf{G}_i = k_i\mathbf{Q} \tag{12}$$

Thereby k_1 and k_2 are unknown scale factors, because $\mathbf{x}^T\mathbf{A}\mathbf{x} = 0$ and $\mathbf{x}^T k\mathbf{A}\mathbf{x} = 0$ describe the same conic.

The basic constraint is then given by:

$$\mathbf{G}_1^T\mathbf{A}_1\mathbf{G}_1 = k_1\mathbf{Q} \quad \text{with} \quad \mathbf{G}_1 = \begin{pmatrix} \mathbf{r}_{11} & \mathbf{r}_{12} & \mathbf{t}_1 \end{pmatrix} \tag{13}$$

$$\mathbf{G}_2^T\mathbf{A}_2\mathbf{G}_2 = k_2\mathbf{Q} \quad \text{with} \quad \mathbf{G}_2 = \begin{pmatrix} \mathbf{r}_{21} & \mathbf{r}_{22} & \mathbf{t}_2 \end{pmatrix} \tag{14}$$

Furthermore the relation between the coordinate systems c_1 and c_2 is known by calibration:

$$\mathbf{R}_2 = \mathbf{R}\mathbf{R}_1 \tag{15}$$

$$\mathbf{t}_2 = \mathbf{R}\mathbf{t}_1 + \mathbf{t} \tag{16}$$

The equations (13) and (14) provide 12 constraints, because they consist of two real symmetric 3×3 matrices with 6 parameters each.

As we only have 10 independent unknowns (three each in $\mathbf{R}_1$ and $\mathbf{t}_1$ as well as k_1, k_2, a and b) the system is overdetermined.

It has been shown that $\mathbf{R}_1$ and $\mathbf{t}_1$ can be solved for independently [14]. With $\mathbf{X}^{2\times2}$ being the upper left submatrix of $\mathbf{X}$ we can write:

$$(\mathbf{R}_1^T\mathbf{A}_1\mathbf{R}_1)^{2\times2} = k_1\mathbf{Q}^{2\times2} \tag{17}$$

$$(\mathbf{R}_2^T\mathbf{A}_2\mathbf{R}_2)^{2\times2} = k_2\mathbf{Q}^{2\times2} \tag{18}$$

Substituting equation (15) into equation (18) we can write after eliminating $\mathbf{Q}^{2\times2}$:

$$[\mathbf{R}_1^T(\mathbf{A}_1 - k\mathbf{R}^T\mathbf{A}_2\mathbf{R})\mathbf{R}_1]^{2\times2} = \begin{pmatrix} 0 & 0 \\ 0 & 0 \end{pmatrix} \text{ with } k = \frac{k_1}{k_2} \tag{19}$$

If the 2×2 upper left submatrix of a 3×3 matrix is equal to a zero matrix, this means that its determinant is equal to zero. Therefore (19) gives:

$$\det(\mathbf{A}_1 - k\mathbf{R}^T\mathbf{A}_2\mathbf{R}) = \det\left[(\mathbf{R}^T\mathbf{A}_2\mathbf{R})^{-1}\mathbf{A}_1 - k\mathbf{E}\right] = 0 \tag{20}$$

This means that k is the eigenvalue of the matrix $(\mathbf{R}^T\mathbf{A}_2\mathbf{R})^{-1}\mathbf{A}_1$. By calculating k and denoting $\mathbf{C} = \mathbf{A}_1 - k\mathbf{R}^T\mathbf{A}_2\mathbf{R}$, equation (19) can be written as:

$$(\mathbf{R}_1^T\mathbf{C}\mathbf{R}_1)^{2\times2} = \begin{pmatrix} 0 & 0 \\ 0 & 0 \end{pmatrix} \tag{21}$$

Equation (21) only provides two independent equations because the matrices are 2×2 symmetric and $\det\mathbf{C} = 0$ has already been used for the solution of k.

Now $\mathbf{R}_1$ can be solved for: One of the eigenvalues of the matrix $\mathbf{C}$ is zero, because $\det(\mathbf{C}) = 0$. Given the two non-zero eigenvalues λ_1 and λ_2 with the corresponding eigenvalues $\mathbf{s}_1$ and $\mathbf{s}_2$ the third column of $\mathbf{R}_1$ can be calculated by:

$$\mathbf{r}_{13} = \pm\text{norm}\left(\sqrt{|\lambda_1|}\mathbf{s}_1 \pm \sqrt{|\lambda_2|}\mathbf{s}_2\right) \tag{22}$$

Here $\text{norm}(\mathbf{x})$ means that $\mathbf{x}$ is normalized to length one. The above case differentiations result in four different possible solutions for $\mathbf{r}_{13}$.

This is due to the fact that two intersecting cones have two shared ellipses. As can be seen from Figure 4 ambiguities can be resolved by considering two cases: In the first case (Figure 4 $\{1\}$) both cameras are on the same side of the ellipse and in the second case (Figure 4 $\{2\}$) one camera is on the front side and the other camera is on the back side of the ellipse. As there is no way to watch a pupil from both sides and we generally want the gaze-vector pointing away from the eyeball, we can rule out three of the solutions by ensuring that the z-components of both $\mathbf{r}_{13}$ and $\mathbf{r}_{23} = \mathbf{R}\mathbf{r}_{13}$ are positive. After having picked the correct $\mathbf{r}_{13}$ the remaining columns of $\mathbf{R}_1$ can be obtained by calculating the eigenvectors $\mathbf{r}_{11}$ and $\mathbf{r}_{12}$ of $\mathbf{H} = \mathbf{r}_{13}^T\mathbf{r}_{13}\mathbf{A}_1$.

Finally, all remaining parameters are solved:

$$\mathbf{R}_2 = \mathbf{R}\mathbf{R}_1; \quad \mathbf{t}_1 = \begin{pmatrix} \mathbf{r}_{11}^T\mathbf{A}_1^T \\ \mathbf{r}_{12}^T\mathbf{A}_1^T \\ \mathbf{r}_{21}^T\mathbf{A}_2^T\mathbf{R} \end{pmatrix}^{-1} \begin{pmatrix} 0 \\ 0 \\ -\mathbf{r}_{21}^T\mathbf{A}_2^T\mathbf{t} \end{pmatrix} \tag{23}$$

$$k_1 = -\mathbf{t}_1^T\mathbf{A}_1\mathbf{t}_1; \quad k_2 = \frac{k}{k_1} \tag{24}$$

$$a^2 = \frac{k_1}{\mathbf{r}_{11}^T\mathbf{A}_1\mathbf{r}_{11}}; \quad b^2 = \frac{k_1}{\mathbf{r}_{12}^T\mathbf{A}_1\mathbf{r}_{12}} \tag{25}$$

3.2. Calibration

One prerequisite is, that the position and orientation of the second camera with respect to the first camera must be known. To get this information, the Camera calibration toolbox for MATLAB has been used. The calibration process involves printing a checkerboard pattern, and taking several pictures of the pattern with both cameras from different angles and distances. An iterative algorithm based on [15] is then used to calculate the intrinsic and extrinsic parameters of both cameras as well as the extrinsic parameters of the stereo rig.

3.3. Hardware and software setup

The system uses calibrated stereo cameras that observe a subject's face sitting about 100 cm away. The scene is illuminated by two infrared LEDs positioned near the optical axis of each camera. This produces the so called red-eye effect, where incoming light is reflected by the blood-rich retina in the direction of the light source which is near the camera. The monochrome cameras have a high sensitivity in the near IR spectrum, so the pupils appear as bright, white spots, just like the red-eye effect in amateur photography.

First, a face tracking algorithm is applied to both input images to find the approximate eye positions. In the area around the assumed eye position a simple thresholding algorithm is applied to roughly find the pupil centers. From there on, the edge points of the pupil are extracted by segmenting the pupil and integrating over the intensity until there is a drop when the darker iris is reached. An ellipse fitting algorithm is applied to the resulting edge points, to get the ellipse parameters of the projected pupil. Figure 5 shows a sample output of the image processing algorithm.

Using this ellipse reconstruction algorithm, the pose of the original pupil surface is then computed in a closed mathematical framework [16] in 3D space relative to the camera coordinate systems. For visualization, a scene view from above is given in Figure 5.

4. RESULTS

Figure 1 shows the implemented camera orientation device mounted on the humanoid robot *JOHNNIE*. The workspace of the device is $\pm 30^\circ$ in the tilt and $\pm 40^\circ$ in the pan direction. This corresponds approximately to the human oculomotor range [1] and is considered sufficient for the intended applications. The weight of the device without cabling is about 140 g including the 11 g of the used firewire camera. With the implemented controller the camera can be oriented with velocities of up to 1000 °/s, which is more than required by human eye movements [1].

In the second application that we mentioned in the Introduction, the camera orientation device is part of a gaze-controlled head-mounted camera (*EyeSeeCam*, see Figure 2). In this configuration, the total system delay between a tracked eye movement and the corresponding movement of the camera is an important measure for system performance. With the new actuation device the total delay amounts to 8 ms, which is on the order of the human vestibulo-ocular reflex [1]. The eye tracking system and the camera orientation device account for 5 ms and 3 ms, respectively, of the delay.

The performance of eye trackers is characterized mainly by the achieved sampling rate as well as by their resolution and accuracy in the space domain. There have been previous attempts to determine gaze from stereo camera configurations [13, 17], however, this is the first application of a closed-form stereo reconstruc-

tion of conics [14] to a remote eye tracking system. Due to the direct calculation of pupil ellipse parameters in a closed-form framework the presented algorithm is real-time capable. There was no degradation of system performance even at the maximum possible frame rate of 500 Hz. While the algorithm ensures superior resolution in the time domain, the resulting resolution in space is not sufficient. We obtained a resolution of 4° (RMS), which is due to the small pupil projections that lead to weakly defined ellipse parameters. This leads to considerable gaze vector variabilities that are not adequate for proper eye tracking.

5. CONCLUSIONS AND OUTLOOK

We have developed a light-weight, wearable and fast camera orientation device that covers and even excels the spatial and dynamical requirements of human ocular motor function. The used piezo actuators proved beneficial in our attempts to reach this goal. This new camera orientation device will find its applications as a robotic vision system and also as the actuation device for a gaze-controlled head-mounted camera system. Future work will focus on further miniaturization. This is required for a new stereo or binocular vision system.

The stereo reconstruction algorithm has prowen useful for the implementation of a novel eye tracker with unprecedented functionality. One drawback, however, is that the ellipse parameters of the conics reconstruction algorithm are not well defined around the primary position. Future work will address this problem by improving the image processing used to extract the pupil contours. In particular, methods of sensor fusion will be investigated, i.e., the ability to operate free of calibration will be combined with existing, but less variable tracking algorithms. The active cameras will be guided by a wide angle face detection system. Based on these results, eye trackers can be designed without the need for a lengthy fixation-based calibration procedure. The closed-form solution of the algorithm guarantees real-time performance even with high sampling rates.

6. ACKNOWLEDGEMENTS

This work was supported in part within the DFG excellence initiative research cluster Cognition for Technical Systems - CoTeSys.

References

[1] J. R. Leigh and D. S. Zee, *The neurology of eye movements*, ser. Contemporary neurology series. Oxford University Press New York, 1999, vol. 55.

[2] J. B. Pelz and R. Canosa, "Oculomotor behavior and perceptual strategies in complex tasks." *Vision Res*, vol. 41, pp. 3587–3596, 2001.

[3] A. E. Patla and J. N. Vickers, "How far ahead do we look when required to step on specific locations in the travel path during locomotion?" *Exp Brain Res*, vol. 148, pp. 133–138, 2003.

[4] M. F. Land, "Eye movements and the control of actions in everyday life." *Prog Retin Eye Res*, vol. 25, pp. 296–324, 2006.

[5] S. R. H. Langton, R. J. Watt, and V. Bruce, "Do the eyes have it? Cues to the direction of social attention." *Trends Cogn Sci*, vol. 4, pp. 50–59, 2000.

[6] U. Castiello, "Understanding other people's actions: intention and attention." *J Exp Psychol Hum Percept Perform*, vol. 29, pp. 416–430, 2003.

[7] T. Shibata, S. Vijayakumar, J. Conradt, and S. Schaal, "Biomimetic oculomotor control," *Adaptive Behavior*, vol. 9, pp. 189–207, 2001.

[8] R. Beira, M. Lopes, M. Praca, J. Santos-Victor, A. Bernardino, G. Metta, F. Becchi, and R. Saltaren, "Design of the robot-cub (icub) head," in *Proceedings of the IEEE International Conference on Robotics and Automation*, May 2006.

[9] E. Schneider, T. Dera, K. Bard, S. Bardins, G. Boening, and T. Brand, "Eye movement driven head-mounted camera: it looks where the eyes look," in *Systems, Man and Cybernetics, 2005 IEEE International Conference on*, vol. 3, 2005, pp. 2437–2442 Vol. 3.

[10] M. Gienger, K. Löffler, and F. Pfeiffer, "Design and realization of jogging johnnie," *CISM Courses and Lectures*, vol. 438, pp. 445–452, 2002.

[11] H. Ulbrich, T. Buschmann, and S. Lohmeier, "'development of the humanoid robot lola," *Applied Mechanics and Materials*, vol. 5-6, pp. 529–539, 2006.

[12] S. Riebe and H. Ulbrich, "Modelling and online computation of the dynamics of a parallel kinematic with six degrees-of-freedom," *Archive of Applied Mechanics (Ingenieur Archiv)*, vol. 72, no. 11, pp. 817–829, Jun. 2003.

[13] D. Beymer and M. Flickner, "Eye gaze tracking using an active stereo head," in *Proc. of the IEEE Conference on Computer Vision and Pattern Recognition*, vol. 2, 2003, pp. 451–458.

[14] S. De Ma, "Conics-based stereo, motion estimation, and pose determination," *International Journal of Computer Vision*, vol. 10, no. 1, pp. 7–25, 1993.

[15] Z. Zhang, "A flexible new technique for camera calibration," *Pattern Analysis and Machine Intelligence, IEEE Transactions on*, vol. 22, no. 11, pp. 1330–1334, 2000.

[16] S. Kohlbecher, T. Poitschke, M. Ablaßmeier, G. Rigoll, S. Bardins, and E. Schneider, "Gaze-vector detection by stereo reconstruction of the pupil contours," *Abstract in Journal of Eye Movement Research*, vol. 1, 2007.

[17] H. G. Wang and E. Sung, "Gaze determination via images of irises," *Image and Vision Computing*, vol. 19, pp. 891–911, 2001.